Super-revivals, chaos, and entanglement of a trapped ion in a standing wave

Mao-Fa Fang,[1,2,3] S. Swain,[2] and Peng Zhou[2,*]
[1]*Department of Physics, Hunan Normal University, Changsha, Hunan 410081, China*
[2]*Department of Applied Mathematics and Theoretical Physics, The Queen's University of Belfast, Belfast BT7 1NN, United Kingdom*
[3]*Anhui Institute of Optics and Fine Mechanics, Academia Sinica, Hefei 230031, China*
(Received 13 October 1999; published 12 December 2000)

We unitarily transform the Hamiltonian of a trapped ion, situated at any position of a standing-wave laser field, to that for the normal Jaynes-Cummings model in the bare ionic basis, and we obtain the general evolution operator of the trapped ion system. We show the existence of super-revivals of the ionic inversion if the trapped ion is *not* located at a node of the standing wave, and we examine the degree of entanglement between the vibrational phonons and the trapped ion. For some parameter values, we find chaotic behavior.

DOI: 10.1103/PhysRevA.63.013812 PACS number(s): 42.50.Ct, 42.50.Vk, 32.90.+a, 03.65.Ta

I. INTRODUCTION

In recent years, much attention has been focused on the dynamics of trapped ions, due to potential applications in the generation of nonclassical states of the vibrational motion of ions [1–3], precision spectroscopy [4], the implementation of quantum logic gates [5], and quantum state reconstruction [6,7]. Although the interaction of a trapped ion with one laser beam or several laser beams is, in general, very complicated, it can be greatly simplified under certain limiting conditions that may indeed be realized in experiments. For example, Cirac *et al.* [1] showed that the dynamics of a trapped two-level ion, at the node of a standing wave, can be described by the Jaynes-Cummings model (JCM). Of late, Wu and Yang [8] and Alam and Bennet [9] extended the study, and predicted that an ion trapped in any position of a laser standing wave, under the conditions of the rotating-wave approximation, the Lamb-Dicke limit, and the strong confinement limit, can also be described by the JCM Hamiltonian, but in an ionic dressed basis. Moya-Cessa *et al.* [10] showed the existence of a unitary transform for the case of an ion interacting with a traveling wave, which transforms the Hamiltonian into a JCM-like form, without making the Lamb-Dicke approximation, and also discussed super-revivals in the phonon number. These works established complete connection between the trapped ion dynamics and cavity QED within the framework of the JCM, and have important implications for both fields.

Here, working within the Lamb-Dicke limit, we introduce a unitary transformation which reduces the Hamiltonian of a trapped ion at any position of a standing wave to that of the normal JCM in the *bare basis* of the trapped ion. Therefore, one can *directly* use the formulas of the standard JCM to study the dynamics of the trapped ion at any position of the standing wave. By means of this transformation, we describe the general evolution of a trapped ion located at an arbitrary point in a standing-wave field, and show that the behavior of the trapped ion depends in a qualitative way on its position in the standing wave field. We consider, in particular, the case where the phonons are initially in a coherent state. If the coherent state is in phase with the driving laser and the trapped ion is not located at a node, the system exhibits the dynamical behavior of super-revivals (revivals which occur on a very long time scale) in the *ionic inversion*. Super-revivals in the photon number were previously reported for the driven JCM in Ref. [11], and by Moya-Cessa *et al.* [10] for their ion system.

If the initial phonon coherent state is out of phase with the driving laser, we find that the system may exhibit chaotic behavior. We also examine the properties of entanglement between the vibrational phonons and the ion in a trapped ion system.

II. MODEL

We consider a single two-level ion, with ground and excited levels $|1\rangle$ and $|2\rangle$, trapped in a harmonic potential of frequency ν and interacting with a standing-wave laser field. In the case where the trap frequency ν is much greater than the ionic decay rate, the Hamiltonian reads[1,8]

$$H=\nu a^{\dagger}a+\frac{\Delta}{2}\sigma_z+\frac{\Omega_0}{2}\sigma_x\cos[\eta(a+a^{\dagger})+\chi], \qquad (1)$$

where a and $a^{\dagger}$ are the annihilation and creation operators of the phonons or vibrational states of the trap; $\Delta=\omega_0-\omega_L$ is the detuning between the ionic transition and laser frequencies; $\sigma_x=\sigma_{21}+\sigma_{12}$ and $\sigma_z=\sigma_{22}-\sigma_{11}$; $\sigma_{ij}=|i\rangle\langle j|$ are the two-level polarization and inversion operators; Ω_0 is the Rabi frequency, which is proportional to the amplitude of the standing wave; η is the Lamb-Dicke parameter; and the phase χ accounts for the relative position of the ion in the standing wave—for example, $\chi=\pi/2$ corresponds to the ion centered at a node of the standing wave. We use units such that $\hbar=1$.

We expand Hamiltonian (1) in powers of the Lamb-Dicke parameter η,

$$H=\nu a^{\dagger}a+\frac{1}{2}\Delta\sigma_z+\frac{1}{2}\Omega_0\cos(\chi)\sigma_x-\eta\frac{\Omega_0}{2}\sin(\chi)\times\sigma_x(a+a^{\dagger})+O(\eta^2), \qquad (2)$$

where terms of higher order in η are negligible in the Lamb-Dicke limit. It is clear that Hamiltonian (2) has the same form as that of a two-level atom coupled to a single quantized cavity field with the coupling coefficient

*Present address: School of Physics, Georgia Institute of Technology, Atlanta, GA 30332.

$-\eta\Omega_0\sin(\chi)/2$, and classically driven by a coherent laser field with Rabi frequency $\Omega_0\cos(\chi)/2$.

We wish to transform Hamiltonian (2) into the JCM Hamiltonian, by eliminating the third term of Eq. (2). This can be achieved by a simple rotation $U=\exp(i\phi\sigma_2)$ about the y axis, where $\tan(2\phi)=\Omega_1/\Omega$ and

$$\Omega=\sqrt{\Delta^2+\Omega_1^2} \quad \text{with} \quad \Omega_1=\Omega_0\cos(\chi). \tag{3}$$

However, we obtain more convenient expressions if we first rotate H through an angle π about the x axis, by application of the unitary operator σ_x, so that the sign of the term in Δ is reversed. We therefore introduce an unitary transform $T=U\sigma_x$, where, explicitly,

$$T=x\sigma_x+y\sigma_z, \tag{4}$$

with

$$x=\left(\frac{\Delta+\Omega}{2\Omega}\right)^{1/2}, \quad y=\frac{\Omega_1}{\sqrt{2\Omega(\Delta+\Omega)}}, \tag{5}$$

which corresponds to an su(2) rotation in the atomic space. Acting with T on the factor $\sigma_x(a+a^\dagger)$ of the fourth term of Eq. (2) introduces an unwanted term proportional to $\sigma_z(a+a^\dagger)$, which, however, is eliminated when the rotating-wave approximation is made, along with terms proportional to $\sigma_{21}a^\dagger$ and $\sigma_{12}a$. In detail, Hamiltonian (2) is transformed by T to

$$H'=THT^\dagger=\nu a^\dagger a+\frac{\Omega}{2}\sigma_z\left[1-\frac{\eta\Omega_0^2\sin(2\chi)}{2\Omega^2}(a+a^\dagger)\right]+\frac{\eta\Omega_0\Delta\sin(\chi)}{2\Omega}\sigma_x(a+a^\dagger). \tag{6}$$

The next step is make the rotating-wave approximation, which involves neglecting those terms in the interaction between the phonons and the atom which do not conserve energy. The primary effect of these neglected terms is to produce a small shift of the atomic frequency. We then find

$$H'=H_{\rm JCM}=\nu a^\dagger a+\frac{\Omega}{2}\sigma_z+g(\sigma_{21}a+\sigma_{12}a^\dagger), \tag{7}$$

where $g=\eta\Omega_0\Delta\sin(\chi)/2\Omega$.

It is clear that the transformed Hamiltonian [Eq. (7)] is formally the same as that of the normal JCM. Therefore, we may directly use the well-known JCM results to study the dynamics of the trapped ion situated at any position of standing wave. For example, if we substitute

$$|\psi'(t)\rangle=\sum_{n=0}^{\infty}[A_n(t)|2,n\rangle+B_n(t)|1,n\rangle] \tag{8}$$

into the Schrödinger equation, $i|\dot{\psi}'(t)\rangle=H'|\psi'(t)\rangle$, where $|j,n\rangle\equiv|j\rangle|n\rangle$, $j=1$ and 2, denotes the state where the atom is in state $|j\rangle$ and there are n photons in the field, we find

$$\begin{pmatrix}A_n(t)\\B_{n+1}(t)\end{pmatrix}=\exp\left[-i\left(n+\frac{1}{2}\right)\nu t\right]\begin{bmatrix}\varepsilon_n & -i\eta_n\\ -i\eta_n & \varepsilon_n^*\end{bmatrix}\times\begin{pmatrix}A_n(0)\\B_{n+1}(0)\end{pmatrix}, \tag{9}$$

where

$$\varepsilon_n=\cos\omega_n t-i\frac{\delta\sin\omega_n t}{2\omega_n}, \qquad \eta_n=\frac{g\sqrt{n+1}\sin\omega_n t}{\omega_n}, \tag{10}$$

with $\omega_n=[\delta^2/4+g^2(n+1)]^{1/2}$ and $\delta=\Omega-\nu$.

Assuming, for example, an initial state in which the atom is in its ground state and the probability amplitude for n phonons to be in the field is F_n,

$$|\psi(0)\rangle=\sum_{n=0}^{\infty}F_n|n,1\rangle, \tag{11}$$

we have $|\psi'(0)\rangle=T|\psi(0)\rangle$, so that

$$A_n(0)=yF_n, \quad B_n(0)=-xF_n. \tag{12}$$

For phonons initially in a coherent state, we have

$$F_n=\exp\left(-\frac{|\alpha|^2}{2}\right)\frac{\alpha^n}{\sqrt{n!}}, \tag{13}$$

where $\alpha=\sqrt{\bar{n}}\exp(i\beta)$, $\bar{n}$ being the initial average phonon number, and β the phase of the phonon coherent state. The mean photon number is $\bar{n}=|\alpha|^2$. Performing the inverse transform on Eq. (8), we obtain

$$|\psi(t)\rangle=T^\dagger|\psi'(t)\rangle=\sum_{n=0}^{\infty}\exp(-in\nu t)[C_n(t)|2,n\rangle+S_n(t)|1,n\rangle]\equiv|C(t)\rangle|2\rangle+|S(t)\rangle|1\rangle, \tag{14}$$

where

$$C_n(t)=\exp(-i\nu t/2)(xy\varepsilon_nF_n+ix^2\eta_nF_{n+1})-\exp(i\nu t/2)\times(xy\varepsilon_{n-1}^*F_n+iy^2\eta_{n-1}F_{n-1}), \tag{15}$$

$$S_n(t)=\exp(-i\nu t/2)(ixy\eta_nF_{n+1}+y^2\varepsilon_nF_n)+\exp(i\nu t/2)\times(ixy\eta_{n-1}F_{n-1}+x^2\varepsilon_{n-1}^*F_n), \tag{16}$$

and

$$|X(t)\rangle=\sum_{n=0}^{\infty}\exp(-in\nu t)X_n(t)|n\rangle, \quad X=C,S. \tag{17}$$

The density matrix of the system is given by

$$\rho(t)=|\psi(t)\rangle\langle\psi(t)| \tag{18}$$

Tracing $\rho(t)$ over the ionic variables gives rise to the reduced phonon density operator,

$$\rho_p(t)=|C\rangle\langle C|+|S\rangle\langle S| \tag{19}$$

It is not difficult to see that its eigenvalues and eigenstates are

$$\Pi^{\pm}(t)=\begin{cases}\langle C|C\rangle \pm \exp(\mp\theta)|\langle C|S\rangle| \\ \langle S|S\rangle \pm \exp(\pm\theta)|\langle C|S\rangle|\end{cases} \tag{20}$$

and

$$|\psi_p^{\pm}\rangle=\frac{1}{\sqrt{\Pi^{\pm}(t)+\Pi^{\mp}\exp(\mp 2\theta)}}(|C\rangle\pm\exp(-i\varphi\mp\theta)|S\rangle), \tag{21}$$

where

$$\theta=\sinh^{-1}\left(\frac{\langle C|C\rangle-\langle S|S\rangle}{2|\langle C|S\rangle|}\right) \tag{22}$$

and

$$\varphi=\tan^{-1}\left[\frac{\mathrm{Im}(\langle C|S\rangle)}{\mathrm{Re}(\langle C|S\rangle)}\right]. \tag{23}$$

Similarly, by tracing over the phonon variables, we find the reduced ionic density operator,

$$\rho_I(t)=\begin{bmatrix}\langle C|C\rangle & \langle S|C\rangle \\ \langle C|S\rangle & \langle S|S\rangle\end{bmatrix}. \tag{24}$$

The eigenvalues $\Pi^{\pm}(t)$ of this operator are identical to the phonon eigenvalues, Eq. (20), and the eigenvectors are

$$|\psi_i^{\pm}\rangle=\frac{1}{\sqrt{\Pi^{\pm}(t)+\Pi^{\mp}\exp(\mp 2\theta)}}(|2\rangle\pm\exp(i\varphi\mp\theta)|1\rangle). \tag{25}$$

In what follows, we shall explore the dynamics of the trapped ion in terms of the quantum collapses and revivals of the ionic inversion, and of the quantum entropy which reflects the degree of entanglement between the internal (ionic) and external (vibrational phonon) degrees of freedom of the trapped ion system. We also find chaotic behavior for certain parameter values.

III. SUPER-REVIVALS OF IONIC INVERSION

From Eq. (24), one obtains the following expression for the inversion of the two-level trapped ion

$$W(t)=\mathrm{Tr}[\rho_I(t)\sigma_z]=\tfrac{1}{2}(\langle C|C\rangle-\langle S|S\rangle). \tag{26}$$

Using Eqs. (17), we find

$$\begin{aligned}W(t)=\tfrac{1}{2}\sum_{n=0}^{\infty}\{&(x^2-y^2)[y^2(|\varepsilon_n|-\eta_n^2)\\&-x^2(|\varepsilon_{n-1}|^2-\eta_{n-1}^2)]|F_n|^2\\&-4xy\,R\{\exp(i\nu t)[iF_n\eta_n(y^2\varepsilon_{n+1}^*F_{n+1}^*\\&-x^2\varepsilon_{n-1}^*F_{n-1}^*)+xy|F_n|^2(\varepsilon_n^*\varepsilon_{n-1}^*+\eta_n\eta_{n+1})]\}\}.\end{aligned} \tag{27}$$

For the case $\chi=\pi/2$, it is clear from Eq. (2) that our Hamiltonian reduces to that of the normal JCM. Then $x=1$ and $y=0$, and Eq. (27) becomes

$$\begin{aligned}W(t)&=-\frac{1}{2}\sum_{n=0}^{\infty}(|\varepsilon_{n-1}|^2-\eta_{n-1}^2)|F_n|^2\\&\rightarrow-\frac{1}{2}\sum_{n=0}^{\infty}\cos(2g\sqrt{n}t)|F_n|^2\quad\text{for }\delta=0.\end{aligned} \tag{28}$$

The above is the standard expression for the inversion in the normal JCM, and it exhibits well-known collapses and revivals for suitable choices of $|F_n|^2$. Analytic expressions have been obtained for these [14,15], where it was shown that the revivals occur at multiples of the revival time, T_R, and that the width of the νth revival is τ_ν, where

$$T_R=2\pi\bar{n}/g,\quad \tau_\nu=2\pi\nu/g\ \ (\nu=1,2,3,...),\quad \tau_0\simeq 3/g \tag{29}$$

for an initial coherent state. When $\chi\neq\pi/2$, the considerably more complicated expression (27) has to be employed.

For simplicity, we consider only the ''resonant'' case $\delta=0$ in the figures. This choice reduces the number of parameters, and ε_n and η_n simplify to $\varepsilon_n=\cos(gt\sqrt{n+1})$ and $\eta_n=\sin(gt\sqrt{n+1})$. Figure 1 presents numerical results for the ionic inversion $W(t)$ for $\Omega_0=6\pi\times10^5\,\mathrm{s}^{-1}$, $\Delta=\Omega_0/20$, $\eta=0.05$, and $\bar{n}=25$ [12], and different positions in the standing wave. This figure shows that the oscillatory features of the inversion strongly depend on the location of the trapped ion in the standing wave, and on the initial vibrational state. We take the initial phonon phase to be $\beta=0$ in the first two frames of Fig. 1. When the trapped ion is located at a node of the standing wave, $\chi=\pi/2$, as in Fig. 1(a), the time behavior of the ionic inversion $W(t)$ exhibits ordinary collapses and revivals. The value of g is $g\simeq4.7\times10^4\,\mathrm{s}^{-1}$. [It should be noted that in general the effective coupling coefficient $g=\eta\Omega_0\Delta\sin(\chi)/2\Omega$ is strongly position dependent.] It can be seen that the collapse occurs after about 7×10^{-5} s, and the revival after about 7×10^{-4} s. These results are in agreement with the expressions in Eq. (29): $T_R\approx6.7\times10^{-4}$ s and $\tau_0\simeq6.4\times10^{-5}$ s. Our system in this case is completely equivalent to the normal JCM.

By contrast, when $\chi=\pi/4$, as in Fig. 1(b), the revivals in the ionic inversion begin from $t\approx1.4$ s. This time is very long compared to that of Fig. 1(a). Such ''super-revivals'' [10,11,13] were previously reported for the photon or phonon number, but not, as far as we are aware, for the inversion. The appearance of the super-revivals can be understood by noting that when $\chi=\pi/4$ and $\Delta\ll\Omega$, then x and y are of

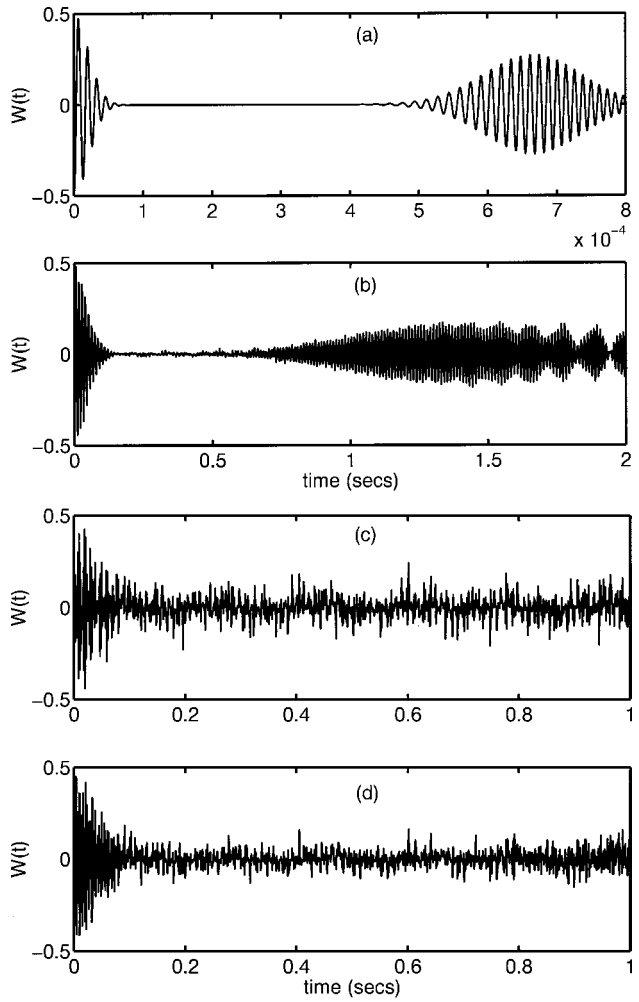

FIG. 1. The time evolution of the ionic inversion $W(t)$ of a trapped ion in a standing-wave field. The ion is initially in the ground state $|1\rangle$, and the vibrational phonons in the coherent state with average phonon number $\bar{n}=25$. $\Omega_0=6\pi\times10^5\,\mathrm{s}^{-1}$, $\Delta=\Omega_0/20$, and $\eta=0.05$. (a) The trapped ion is located at the node of the standing wave, $\chi=\pi/2$ and $\beta=0$. (b) The trapped ion is midway between node and antinode of the standing wave. $\chi=\pi/4$ and $\beta=0$. (c) The trapped ion is midway between node and antinode of the standing wave, $\chi=\pi/4$, but now with a nonzero coherent state phase, $\beta=\pi/2$. (d) The trapped ion is midway between node and antinode of the standing wave, but now $\chi=\pi/4$ and $\beta=\pi/4$.

nearly equal magnitude. Thus the first term in Eq. (27), which was responsible for all the contributions for the case of Fig. 1(a), the normal JCM, is now small, and it is the second term of Eq. (27) which makes the major contribution. This term contains factors such as $\varepsilon_n^*\varepsilon_{n-1}^*=\cos(g\sqrt{n+1}t)\cos(g\sqrt{n}t)=\frac{1}{2}\{\cos[g(\sqrt{n+1}+\sqrt{n})t]+\cos g[(\sqrt{n+1}-\sqrt{n})t]\}$. The first term, with a time argument of approximately $2g\sqrt{n}t$ for large n, is essentially the time argument that arises in Eq. (28) which determines Fig. 1(a), but the second term, with a time argument of approximately $1/2gt/\sqrt{n}$, evolves over a much longer time scale. The ratio between these two time scales, for $n\simeq\bar{n}$, is $4\bar{n}$, and the time at which the super-revival occurs is $T_{\mathrm{SR}}=4\bar{n}T_R$.

To see this more clearly, we approximate the terms in Eq. (27), assuming that $n\gg1$, and retain only terms to lowest significant order in $\sqrt{n}$. We obtain

$$W(t)=\frac{1}{2}\sum_{n=0}^{\infty}\left\{-\frac{\Delta^2}{\Omega^2}\cos 2gt\sqrt{n}-\frac{\Omega_1}{\Omega_2}\times\left[iF_n\left(\frac{\Omega_1^2F_{n+1}^*}{2(\Delta+\Omega)}-(\Delta+\Omega)F_{n-1}^*\right)\right]\sin 2gt\sqrt{n}+\frac{\Omega_1}{\Omega^2}\left[iF_n\left(\frac{\Omega_1^2F_{n+1}^*}{2(\Delta+\Omega)}+(\Delta+\Omega)F_{n-1}^*\right)\right]\sin\frac{gt}{2\sqrt{\pi}}-\Omega_1|F_n|^2\cos\frac{gt}{2\sqrt{\pi}}\right\}. \tag{30}$$

For $\chi=\pi/4$, $\beta=0$, and $\Delta\ll\Omega$, the first two terms in Eq. (30) are small. The dominant contribution comes from the last two terms. For the coherent state [eq. (13)] and for $n\simeq\bar{n}\gg1$, we have

$$F_{n+1}=\frac{\alpha}{\sqrt{\bar{n}}}F_n,\quad F_{n-1}=\frac{\sqrt{\bar{n}}}{\alpha}F_n, \tag{31}$$

so that, for α real, we can roughly approximate $W(t)$ by

$$W(t)=-\frac{A}{2}\sum_{n=0}^{\infty}F_n^2\cos\left(\frac{gt}{2\sqrt{n}}+B\right) \tag{32}$$

[using the last two terms of Eq. (30) only], where A and B are constants. By comparison with Eq. (28), we see that the system behaves like the ordinary JCM, but with the time argument replaced according to the rule

$$2gt\sqrt{n}\rightarrow\frac{gt}{2\sqrt{n}}. \tag{33}$$

The arguments of Sec. II of Ref. [15] can be used to show that the revivals occur with the time

$$T_{\mathrm{SR}}=\frac{8\pi\bar{n}^{3/2}}{g}=4\bar{n}T_R. \tag{34}$$

and their widths are given by

$$\tau_{\mathrm{SR}\nu}=\frac{12\pi\bar{n}\nu}{g},\quad \nu=1,2,3,\ldots,\quad \tau_{\mathrm{SR}0}=\frac{12\bar{n}}{g}. \tag{35}$$

For the parameters of Fig. 1(b), $g\simeq2.3\times10^3\,\mathrm{s}^{-1}$, $T_R\simeq0.013\,\mathrm{s}$, and $T_{\mathrm{SR}}\simeq1.34\,\mathrm{s}$. The latter number is in agreement with the observed revival in the figure. A feature not apparent in the figure is that the first decay exhibits very small-amplitude modulations with period T_R, which arise from the terms neglected in approximating Eq. (30) by Eq. (32). [One requires a plot over a very small time scale to see these.] The width of the first two revivals are found to $\tau_{\mathrm{SR}1}$

$\simeq 0.41$ s and $\tau_{SR2} \simeq 0.82$ s. We thus observe only one revival, as the second revival overlaps the first, giving rise to interference features. The existence of super-revivals in the ionic inversion is a manifestation of the position dependence of the ionic dynamics.

The super-revival time [Eq. (34)] is identical to the fractional revival time introduced by Averbukh [16]. However, the super-revivals described are a different physical phenomena. The second set of terms in Eq. (27) play an essential role in the super-revivals discussed here, whereas the fractional revivals occur in the normal JCM, described by Eq. (28), but with a more sharply peaked photon distribution than that provided by the coherent state [17].

In Figs. 1(c) and 1(d), the ion is placed midway between node and antinode as in Fig. 1(b), but now we allow a nonzero value for the phase of the initial coherent state of the phonons. In Fig. 1(c), we take $\beta = \pi/2$, and in Fig. 1(d) we take $\beta = \pi/4$. In both cases, the inversion appears to show a chaotic behavior, with no indications of revivals or any other regular structure. The introduction of the extra phase factors when $\beta \neq 0$ destroys the interference effects that give rise to collapses and revivals.

IV. ENTANGLEMENT BETWEEN THE VIBRATIONAL PHONONS AND ION

The quantum dynamics described by the Hamiltonian [Eq. (2)] leads to an entanglement between the phonon subsystem and the ion subsystem dressed by the standing wave. Here we use quantum entropy as a measure of the degree of the entanglement, according to the theory presented by Phoenix and Knight [18]. In the trapped ion system, the time behavior of the phonon (or ionic) quantum entropy reflects the time behavior of the degree of entanglement between the phonons and ion. The larger the entropy, the greater the entanglement. The entropies of the phonons and ion can be defined through their respective reduced density operators by

$$S_j(t) = -\mathrm{Tr}_j(\rho_j \ln \rho_j), \tag{36}$$

and the subscript j is taken to imply either the phonons or the ion, or the whole phonon-ion system. The entropies of a general two-component quantum system are linked by a remarkable theorem due to Araki and Lieb [19], which states

$$|S_i(t) - S_p(t)| \leqslant S \leqslant S_i(t) + S_p(t). \tag{37}$$

The subscripts p and i denote the phonons and ion, and the total entropy of the complete p-i system is denoted by S. Since we have assumed the phonons and ion are initially in a disentangled pure state, that is, the phonons are in the vibrational coherent state $|\alpha\rangle$ and the ion in the ground state $|1\rangle$, the entropy S of the complete i-p system is zero. One immediate consequence of the inequality (37) is that the phonon and ion component systems have equal entropies throughout their subsequent evolution: $S_i(t) = S_p(t)$. Hence we calculate only the phonon entropy $S_p(t)$. We may express the phonon entropy in terms of the eigenvalues $\Pi^{\pm}(t)$ of the reduced phonon density operator, given by Eq. (20), as

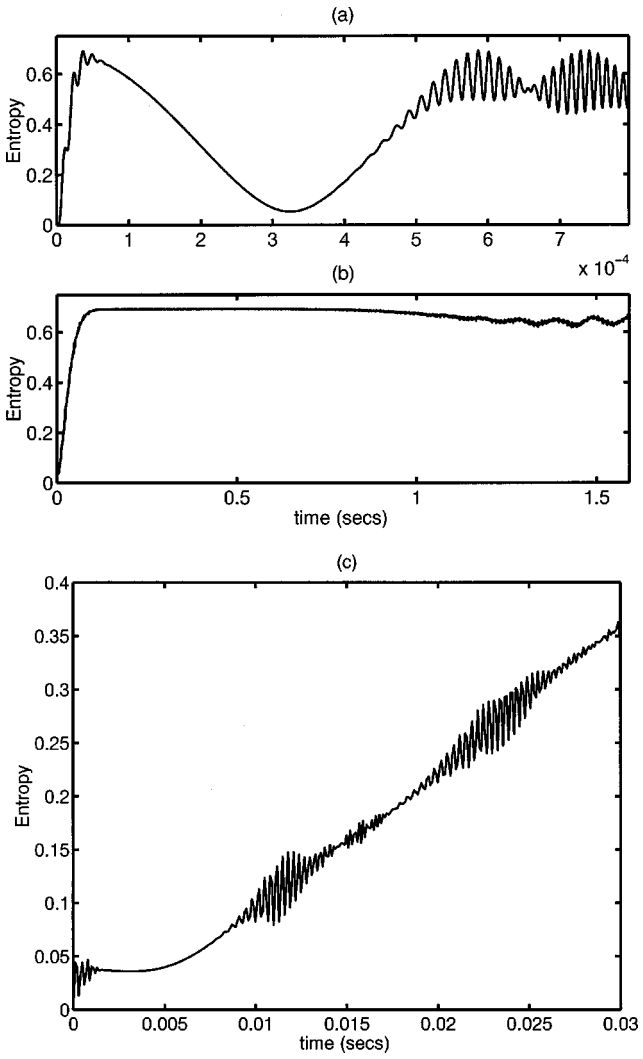

FIG. 2. The time evolution of the phonon entropy of a trapped ion in the standing wave. The parameters are the same as in Fig. 1. (a) The trapped ion is located at the node of the standing wave, $\chi = \pi/2$ and $\beta = 0$. (b) The trapped ion is midway between node and antinode, $\chi = \pi/4$ and $\beta = 0$. (c) shows the early evolution of (b) on a much expanded scale.

$$S_p(t) = -\Pi^+(t)\ln \Pi^+(t) - \Pi^-(t)\ln \Pi^-(t). \tag{38}$$

The numerical results for the entropic evolution of the vibrational phonons are presented in Fig. 2. Here the parameter values are the same as in Fig. 1. In Fig. 2(a), the case where the trapped ion is located at the node of the standing wave ($\chi = \pi/2$) is considered. The evolution of the phonon entropy is the same as that of the field entropy in the JCM. During the first stage of the time evolution, the phonon entropy achieves its maximum value, which means that phonons and ion are strongly entangled; however, at one half of the revival time for the ionic inversion ($t_0 = T_R/2 = 5\pi/g$) the phonon entropy evolves to its local minimum value, which means that the phonons and ion are disentangled and the phonons are in an almost pure state. This pure state is a Schrödinger cat state according to the dynamical properties of the JCM [20]. This demonstrates that Schrödinger cat

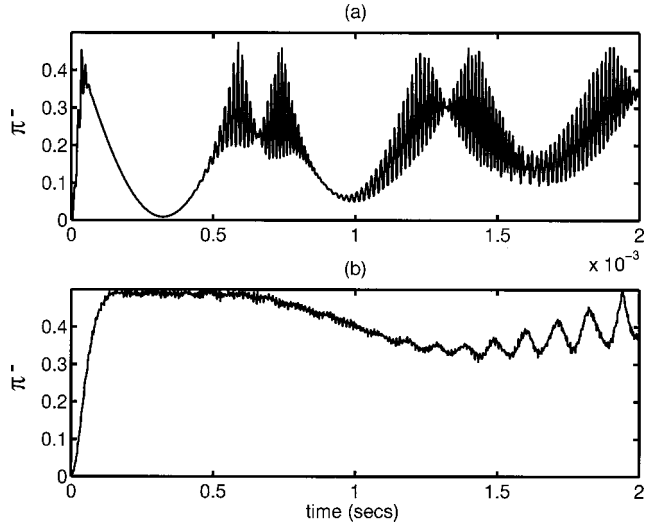

FIG. 3. The time evolution of the eigenvalue $\Pi_p^-(t)$ with the same parameters as in Fig. 1. (a) The trapped ion is located at a node, $\chi=\pi/2$ and $\beta=0$ (b) The trapped ion is midway between node and antinode, $\chi=\pi/4$ and $\beta=0$

states in the motion of a trapped ion can be generated by the phonon-ion interaction. Figure 2(b) shows the case in which the trapped ion is placed away from the node of the standing wave ($\chi=\pi/4$). It is obvious that at very early stages of the time evolution, the phonon entropy remains near its local minimum value, which shows that the phonons and ion are disentangled. As the time goes on, the phonon entropy increases to its maximum value, and the phonons and ion become strongly entangled. A plateau persists for a long time before a slow reduction, and oscillation begins after about 1 s. Figure 2(c) shows the early evolution of Fig. 2(b) on a much expanded scale. The short-time revivals seen here are the ''normal'' JCM revivals, occurring at $T_R\simeq 2\pi\bar{n}^{1/2}/g$.

We may interpret the dynamical behavior of the phonon entropy in terms of the evolution of the state vector of the trapped ion system. By using the eigenvalues and eigenstates of the reduced-density operators of phonons and ion, given by eqs. (20) and (24), we can write the evolution of the ion-phonon system state vector as [18]

$$|\Psi_{i\text{-}p}(t)\rangle=\sqrt{\Pi^+(t)}|\psi_p^+\rangle\otimes|\psi_i^+\rangle+\sqrt{\Pi^-(t)}|\psi_p^-\rangle\otimes|\psi_i^-\rangle. \tag{39}$$

The eigenvalue $\Pi^-(t)$ is plotted in Fig. 3 for $\Omega_0=6\pi\times10^5\,\mathrm{s}^{-1}$, $\Delta=\Omega_0/20$, $\eta=0.05$, and $\bar{n}=25$. [Note that $\Pi^+(t)=1-\Pi^-(t)$.] For the trapped ion located at the node of the standing wave, $\chi=\pi/2$, depicted in Fig. 3(a), $\Pi^-(t)$ tends to zero at t_0, one-half of the revival time of ionic inversion. From Eq. (39), we have

$$\Psi_{i\text{-}p}(t_0)\approx|\psi_p^+\rangle\otimes|\psi_i^+\rangle, \tag{40}$$

that is, the phonons and ion are disentangled and their respective entropy achieves its local minimum value at this time. At all other times, neither $\Pi^+(t)$ or $\Pi^-(t)$ is zero. From Eq. (39), we see that the phonons and ion are always entangled, so that the values of their respective entropies no longer tend to zero. For a trapped ion away from the node of the standing wave, $\chi=\pi/4$, shown in Fig. 3(b), we see that at the early stage of the time evolution, the eigenvalue $\Pi^-(t)$ tends to zero. In this region, the phonons and ion are disentangled, and the phonon entropy has its minimum value. In the collapse region however, $\Pi^+(t)$ and $\Pi^-(t)$ have almost the same value, i.e., $\Pi^+(t)=\Pi^-(t)\approx0.5$, so that the phonons and ion are in an optimally entangled state, and the phonon entropy evolves to its maximum value. It is important to stress that, by using the properties of the entanglement between the phonons and the ion, one can obtain information concerning the phonons by a measurement performed on the ion. When the phonons and ion are in an optimally entangled state, the quality of the information obtained about the phonons from measurements of ionic properties is correspondingly optimal. For example, full information on the quantum-mechanical state of the vibrational center-of-mass motion of a trapped ion can be obtained from the dynamics of the ionic ground state of a long-lived electronic transition [6].

In conclusion, by performing a unitary transformation, we have transformed the Hamiltonian of a trapped ion situated at any position in a standing wave field to that of the normal Jaynes-Cummings model in the bare ionic basis, and we have obtained the general evolution operator of the trapped ion system. We have shown the existence of super-revivals in the ionic inversion if the trapped ion is not located at the node of the standing wave. Since dissipation in traps is much smaller than in cavities, it may be possible to experimentally observe the super-revivals of a trapped ion in a standing wave. We have also examined the properties of entanglement between the vibrational phonons and the trapped ion in terms of quantum entropy.

ACKNOWLEDGMENTS

M.F.F. thanks the Department of Applied Mathematics and Theoretical Physics of the Queen's University of Belfast for hospitality. This work was supported by the National Natural Science Foundation of China and the United Kingdom EPSRC.

[1] D. J. Heinzen and D. J. Wineland, Phys. Rev. A **42**, 2977 (1990); J. I. Cirac, R. Blatt, A. S. Parkins, and P. Zoller, Phys. Rev. Lett. **70**, 762 (1993); J. I. Cirac, A. S. Parkins, R. Blatt, and P. Zoller, Adv. At., Mol., Opt. Phys. **37**, 237 (1996), and references therein.

[2] D. J. Heinzen and D. J. Wineland, Phys. Rev. A **42**, 2977 (1990); R. L. de Matos Filho and W. Vogel, Phys. Rev. Lett. **76**, 608 (1996).

[3] C. C. Gerry, S.-C. Gou and J. Steinbach, Phys. Rev. A **55**, 630 (1997); **55**, 2478 (1997).

[4] D. J. Wineland, J. J. Bollinger, W. M. Itano, F. L. Moore, and D. J. Heinzen, Phys. Rev. A **46**, R6797 (1992).

[5] C. Monroe, D. M. Meekhof, B. E. King, W. M. Itano, and D. J. Wineland, Phys. Rev. Lett. **75**, 4714 (1995); J. I. Cirac and

P. Zoller, *ibid.* **74**, 4091 (1995).
[6] S. Wallentowitz and W. Vogel, Phys. Rev. Lett. **75**, 2932 (1995); J. F. Poyatos, R. Walser, J. I. Cirac, P. Zoller, and R. Blatt, Phys. Rev. A **53**, R1966 (1996); C. D'Helon and G. J. Milburn, *ibid.* **54**, R25 (1996).
[7] D. Leibfried, D. M. Meekhof, B. E. King, C. Monroe, W. M. Itano, and D. J. Wineland, Phys. Rev. Lett. **77**, 4281 (1996).
[8] Y. Wu and X. X. Yang, Phys. Rev. Lett. **78**, 3086 (1997).
[9] S. Alam and C. Bentley, Prog. Theor. Phys. **98**, 351 (1997).
[10] H. Moya-Cessa, A. Vidiella-Barranco, J. A. Roversi, D. S. Freitas, and S. M. Dutra, Phys. Rev. A **59**, 2518 (1999).
[11] S. M. Dutra, P. L. Knight, and H. Moya-Cessa, Phys. Rev. A **49**, 1993 (1994).
[12] J. I. Cirac, R. Blatt, A. S. Parkins, and P. Zoller, Phys. Rev. A **49**, 1202 (1994).
[13] The phenomenon of long-time scaled revivals was termed a ''super-revival'' by A. Venugopalan and G. S. Agarwal, Phys. Rev. A **59**, 1413 (1999).
[14] J. H. Eberly, N. B. Narozhny, and J. J. Sanchez-Mondragon, Phys. Rev. Lett. **44**, 1323 (1980); B. W. Shore and P. L. Knight, J. Mod. Opt. **40**, 1195 (1993); M. O. Scully and M. S. Zubairy, *Quantum Optics* (Cambridge University Press, Cambridge, 1997), Chap. 6; J-S. Peng and G-X. Li, *Introduction to Modern Quantum Optics* (World Scientific, Singapore, 1998).
[15] M. Fleischhauer and W. P. Schleich, Phys. Rev. A **47**, 4258 (1993).
[16] I. Sh. Averbukh, Phys. Rev. A **46**, R2205 (1992).
[17] P. F. Góra and C. Jedrzejek, Phys. Rev. A **48**, 3291 (1993).
[18] S. J. D. Phoenix and P. L. Knight, Ann. Phys. (N.Y.) **186**, 381 (1988); Phys. Rev. Lett. **66**, 2833 (1991); Phys. Rev. A **44**, 6023 (1991).
[19] H. Araki and E. Lieb, Commun. Math. Phys. **18**, 160 (1970).
[20] J. Gea-Banancloche, Phys. Rev. A **44**, 5913 (1991); Phys. Rev. Lett. **65**, 3385 (1990).